Environmental Engineering and Management Journal

August 2020, Vol. 19, No.8, 1261-1268
http://www.eemj.icpm.tuiasi.ro/; http://www.eemj.eu

"Gheorghe Asachi" Technical University of Iasi, Romania

PHOTOCATALYTIC DEGRADATION OF DISPERSE BLUE 56 BY Cu-Ti-PILCs AND Fe-Ti-PILCs

Beytullah Eren[1], Can Serkan Keskin*, Abdil Özdemir[2]

[1]Sakarya University, Faculty of Engineering, Department of Environmental Chemistry, Sakarya, Turkey
[2]Sakarya University, Faculty of Arts and Sciences, Department of Chemistry, Sakarya, Turkey

Abstract

Pollution with aromatic hydrocarbon has been rising because of the extreme usage of benzene containing compounds. Most of the people, animals and plants have been exposed to aromatic hydrocarbons due to polluted water sources. The aim of the present work was to carry out an experimental study for the photocatalytic degradation of aromatic hydrocarbon containing compounds by iron-titanium-pillared interlayered clays (Fe-Ti-PILCs) and copper-titanium-pillared interlayered clays (Cu-Ti-PILCs). For this purpose, a dye named disperse blue 56 (DB56) was selected for treatment experiment. Zeolite was used as a catalyst support material to prepare Fe-Ti-PILCs and Cu-Ti-PILCs. The experiments were carried out in batch method and UV-Vis spectroscopy was used for analysis. Several parameters such as contact time, H_2O_2 and amount of PILCs were examined to find optimized conditions. The obtained degradation rates using Cu-Ti-PILCs were better than Fe-Ti-PILCs. The obtained highest removal rates were ~97% and ~94% for Cu-Ti-PILCs and Fe-Ti-PILCs, respectively in 120 min reaction time with using 100 mg/L of dye, 1 g of Fe-Ti-PILC and Cu-Ti-PILCs and 1 mL of H_2O_2.

Key words: anthraquinone dye, degradation, disperse blue 56, UV radiation, zeolite

Received: November, 2019; Revised final: February, 2020; Accepted: April, 2020; Published in final edited form: August, 2020

1. Introduction

Removal of harmful materials from water is one of the most important application to protect natural life. The natural ground and/or surface water supplies have been polluted by organic compounds. Worldwide, there are millions of people do not have access to clean water. The water quality has been affected by agricultural, industrial applications and urbanization. Drugs, dyes, pesticides, herbicides, surfactants, antimicrobials, natural steroids were the main contaminants reported by researchers (Levine et al., 2006).

DB56 is a dye from anthraquinone class. The anthraquinone compounds have three fused aromatic rings and two keto groups. They are used as dyes and electrochromic materials (Cysewski and Jeliński, 2013). The anthraquinone dyes are second most common class after azo dyes (Dos Santos et al., 2005). These type of dyes are much difficult to degrade and toxic compared to the azo dyes (Fu et al., 2009; Parmar and Shukla, 2018). Different photocatalytic material based methods can be used for wastewater treatment. Enesca et al. (2009) prepared TiO_2 thin film layers via spray pyrolysis deposition with using different quantities and kinds polymers additives for the photocatalytic process. Methyl orange and methyl blue dye solutions were used for photocatalytic degradation tests. They stated that 25 mg/L hydrophobic copolymer added TiO_2 film had higher photodegradation efficiency. Apostolescu et al. (2015) used CeO_2-ZnO polycrystalline material as catalyst for the photocatalytic degradation of methylene blue under UV irradiation. Simion et al. (2015) investigated photocatalytic degradation of Rhodamine 6G dye by photo-Fenton technique in the presence of H_2O_2. They

* Author to whom all correspondence should be addressed: e-mail: ckeskin@sakarya.edu.tr; Phone: +90 2642956036

reported higher degradation efficiencies. Favier et al. (2015) used TiO_2 catalyst for the degradation of carbamazepine and achieved about 87% degradation yield. Caliman et al. (2007) reported degradation of Alcian Blue 8 GX dye by H_2O_2/UV-B and photo-Fenton methods. Wali et al. (2019) used Pd-Ag nanoparticles/macro porous silicon structure for the photocatalytic degradation of methylene blue. The reported maximum photocatalytic efficiency was 98.8%. Aboelenin et al. (2017) investigated catalytic performance of mesoporous silicates derived from natural diatomite and oxidation studies were performed for methylene blue dye in presence of H_2O_2. They reported that mesoporous silicate showed better catalytic activity than mesoporous silicate with CTAB surfactant and modified mesoporous silicate with iron oxides. Also, there are some studies in the literature about degradation of DB56. Zeng et al. (2009) reported NaClO oxidation process under the UV radiation. The stated color removal rate was 100%. Fu et al. (2010) used manganese minerals and UV radiation for the degradation process. The reported color removal efficiency was 94%. Keshmirizadeh and Farajikhajehghiasi (2014) investigated oxidative discoloration of DB56 by Fenton process. The obtained efficiency was 99%. No studies have been found about degradation of DB56 by Ti-PILCs. Therefore, literature reports good efficiency of dyes photocatalytic degradation.

Clays have been used in many adsorption studies owing to porous structure and cheapness. In recent times, they have been used as catalyst support materials due to the appropriate structure. These materials, called Pillared Interlayered Clays, PILCs, have better pore structure than clays. They are usually prepared by the cation exchange method. Immobilization of metal ions such as aluminum, zirconium, iron, zinc and especially titanium, in the interlamellar spaces provide interlayer spaces for adsorption and catalysis (Mnasri et al., 2017). It is difficult to remove or recover a catalyst from reaction medium. The disposal of these catalysts, which may be toxic, causes environmental pollution and also increases the cost of the reaction (Baloyi et al., 2018). These problems can be solved using PILCs. Catalysts can be easily recovered and reused with the use of PILCs. Such studies are known as "green chemistry" because they are not disposed to the environment. Zeolite minerals can also be used for PILCs production.

This paper describes photocatalytic degradation of DB56 by Cu-Ti-PILCs and Fe-Ti-PILCs under UV irradiation. Iron modified Ti-PILCs were commonly used for photocatalytic degradation studies. The main goal of this work was to compare photocatalytic activity of Cu-Ti-PILCs and Fe-Ti-PILCs over an aromatic hydrocarbon. UV-Vis spectroscopy was used to determination of treated solutions concentrations. The morphology of synthesized material was taken by scanning electron microscopy (SEM). Also, FTIR, EDS and XRD analysis were performed to better understand to the structures.

2. Material and methods

2.1. Synthesis of Cu-Ti-PILCs and Fe-Ti_PILCs

The preparation of Cu-Ti-PILCs and Fe-Ti-PILC was carried out according to the previously described method by Carriazo et al. (2010). The intercalating solution was prepared by addition of 60 mL $TiCl_4$ (Merck Chemicals) to the concentrated HCl solution. The solution was diluted with distilled water to 300 mL and stirred for 18 h and obtained ~1.82 M Ti solution. Then, the solution was mixed with 0.5 M of $Fe(NO_3)_3$ (Merck Chemicals) or $Cu(NO_3)_2$ (Merck Chemicals) solution and aged for 24 h. Zeolite was dispersed in 1 L of distilled water and stirred for 24 h. The prepared Fe-Ti or Cu-Ti solution was slowly added to zeolite suspension and stirred for 48 h. The final sample was dried in a water bath until the dryness and then calcined at 400°C for 2 h. The prepared Cu-Ti-PILCs and Fe-Ti-PILCs were grinded in mortar and stored in a desiccator.

2.2. Degradation experiments

The experiments were carried out in a beaker with 100 mL of DB56 solution. Fe-Ti-PILCs or Cu-Ti-PILCs and DB56 solution were stirred by a magnetic stirrer under a UV light from a Black Ray model B-100, UVP Inc. mercury lamp (365 nm maximum wavelength). The samples were centrifuged before UV analysis.

The effect of H_2O_2 was investigated using 0.1 - 10.0 mL of H_2O_2 (50%). Different concentrations of dye (10 - 100 mg/L) and synthesized PILCs amount (0.5 - 3.0 g) were also used to see degradation capacities of Cu-Ti-PILCs and Fe-Ti-PILCs.

2.3. Terephthalic acid photoluminescence test

A volume of 250 mL of 5×10^{-3} M sodium terephthalate was prepared in stoichiometric amount NaOH solution. The experiment for the detection of the hydroxyl radicals was carried out by using 1 g Cu-Ti-PILCs, 100 mL of M sodium terephthalate and 1 mL of H_2O_2. The excitation wavelength of formed hydroxy terephthalate was 315 nm. The fluorescence intensity was measured at 425 nm.

2.4. Characterization

FTIR analyses of zeolite, Fe-Ti-PILCs and Cu-Ti-PILCs were performed using Schimadzu IR Prestige 21 by ATR technique. The morphological characterizations of zeolite and synthesized Cu-Ti-PILCs and Fe-Ti-PILCs were performed by SEM JEOL (JSM- 6060LV) microscope. X-ray diffraction (XRD) patterns of zeolite, Cu-Ti-PILCs and Fe-Ti-PILCs were recorded by Rigaku D/Max 2200

equipped with graphite monochromatized Cu Kα radiation (λ = 1.5406 Å).

3. Results and discussion

In synthesis, metal ions (Cu^{2+} or Fe^{3+}) and titanium containing solution was added to dispersed zeolite suspension. Zeolite was delaminated by forming TiO_2 in the interlayer spaces of clay and modified by metal ions via cation exchange (Carriazo et al., 2010). The FTIR (Fig. 1) and XRD (Fig. 2) results supports this situation. In the FTIR spectrum of zeolite, the band at 1019 cm^{-1} was attributed to asymmetric stretching of -Si-O-Si- and -Si-O-Al groups. The secondary building unit rings of zeolite stretching vibration band appeared at 792 cm^{-1} at zeolite spectrum. Also, the bands at 727 cm^{-1} and 673 cm^{-1} were assigned to symmetric vibration of -Si-O-Si- and -Si-O-Al-, respectively (Byrappa and Suresh Kumar, 2007; Mozgawa et al., 2011). These symmetric vibration bands were disappeared in the spectrum of Cu-Ti-PILCs and Fe-Ti-PILCs. The intensity of asymmetric stretching band decreased and shifted to 1072 cm^{-1} due to cation exchange between aluminum and copper (or iron) ions. The peak at 1630 cm^{-1} resulting from carbonates in the zeolite disappeared in Cu-Ti-PILCs and Fe-Ti-PILCs spectra because of high acidic media while in synthesis process (Stevens et al., 2008).

XRD patterns of zeolite, Cu-Ti-PILCs and Fe-Ti-PILCs are shown in Fig. 2. According to diffraction pattern of zeolite, the type of used zeolite was clinoptilolite [$(NaKCa)_6(SiAl_{36})O_{72}$] (Mansouri et al., 2013; Treacy and Higgins, 2001). The characteristic peaks (2θ) of clinoptilolite appeared at 9.98° and 22.50° (Narváez et al., 2015).

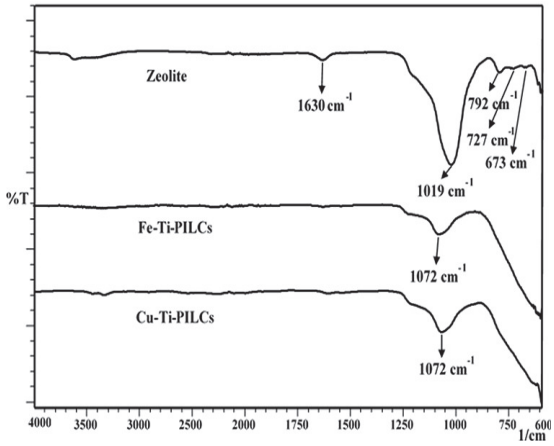

Fig. 1. FTIR spectra of zeolite, Fe-Ti-PILCs and Cu-Ti-PILCs

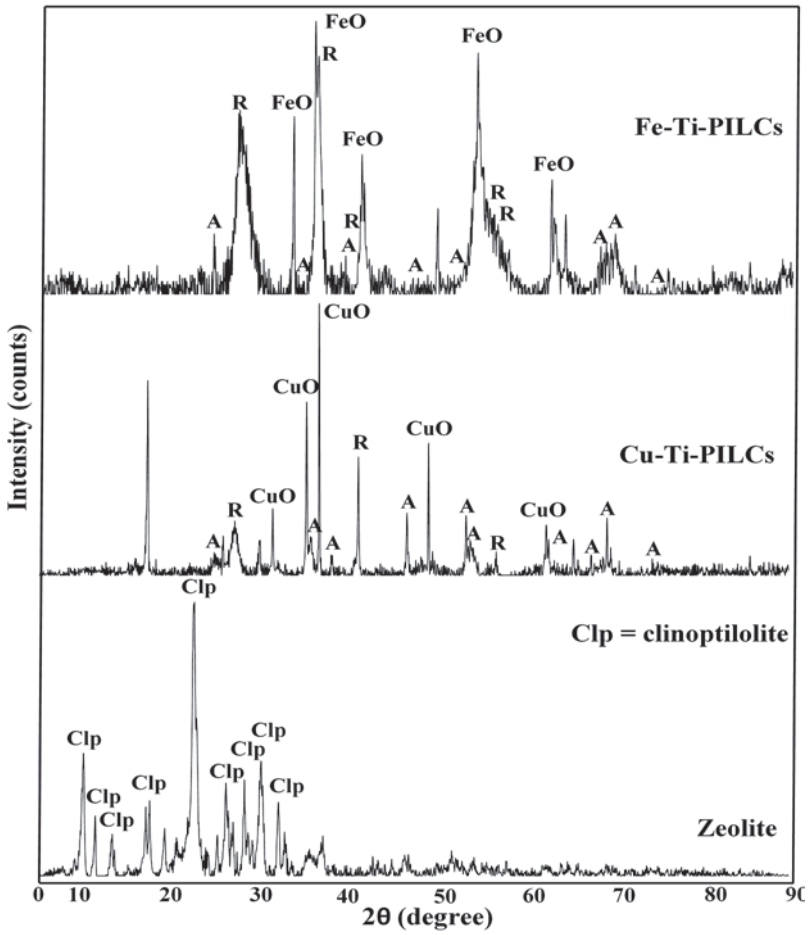

Fig. 2. XRD patterns of zeolite, Fe-Ti-PILCs and Cu-Ti-PILCs

These peaks disappeared or shifted to the lower theta degrees at Cu-Ti-PILCs and Fe-Ti-PILCs XRD patterns. This indicating that the clinoptilolite structure was delaminated (Carriazo et al., 2010). The diffraction peaks appeared at 35.88° and 37.32° in the Cu-Ti-PILCs XRD pattern, were caused by the formed CuO as a result of calcination (Volanti et al., 2008). Similarly, the iron oxides peaks appeared at 35.86° and 54.28° in the Fe-Ti-PILCs XRD pattern (Khalil, 2015; Veintemillas-Verdaguer et al., 2004). The characteristic diffraction peaks of anatase form of TiO_2 were 25.3°, 36.9°, 37.7° 38.6°, 47.9°, 53.8°, 55°, 62.6°,68.8°, 70°, and 74.9° can be assigned to the (1 0 1), (1 0 3), (0 0 4), (1 1 2), (2 0 0), (1 0 5), (2 1 1), (2 0 4), (1 1 6), (2 2 0) and (2 1 5) planes, respectively. The peaks at 27.3°, 36°, 41.1°, 55.1°, and 56.2° can be assigned to the (1 1 0), (1 0 1), (1 1 1), (2 1 1), and (2 2 0) planes of rutile TiO_2. (Islam et al., 2020). As can be seen from Fig. 2, the synthesized PILCs contained both of anatase and rutile form of TiO_2. Cu-Ti-PILCs contained more anatase form than Fe-Ti-PILCs. Thus, Cu-Ti-PILCs showed better photo catalytic activity.

SEM images and EDS patterns are shown in Fig. 3a-f. The EDS pattern of zeolite was consistent with clinoptilolite structure (Monge-Amaya et al., 2013). SEM images showed that Cu-Ti-PILCs and Fe-Ti-PILCs samples comprised of aggregates of particles.

There is no homogeneous sphericity was observed due to zeolite structure at the images. The spherical copper, iron and titanium oxides could be seen on the zeolite structures. The results also proved that Cu-Ti-PILCs and Fe-Ti-PILCs contained copper and iron, respectively. In addition, the EDS results indicates that small amount of Al was still remaining in the structures.

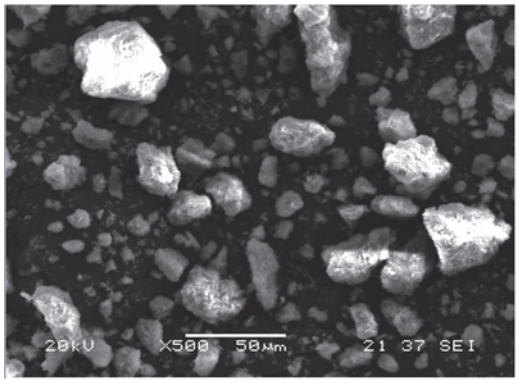

(a)

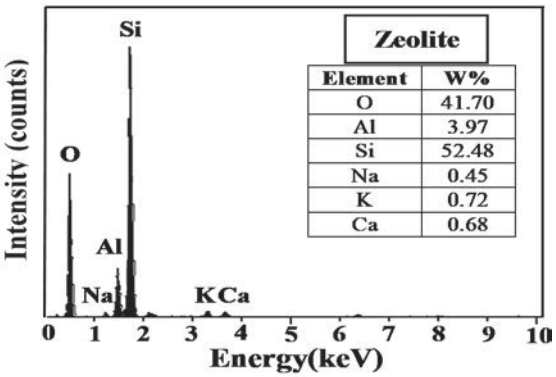

(b)

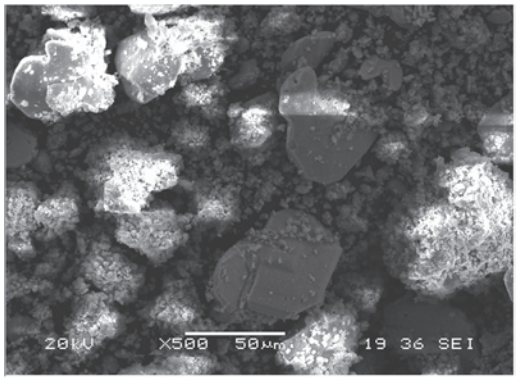

(c)

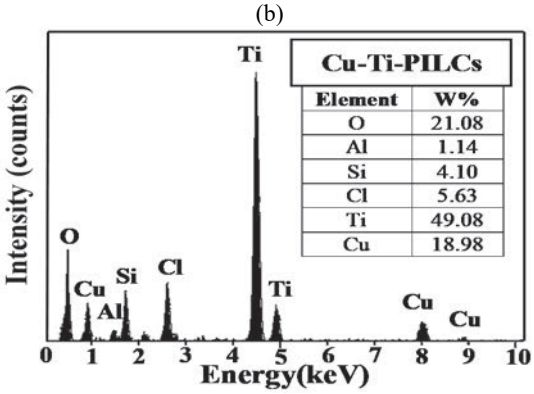

(d)

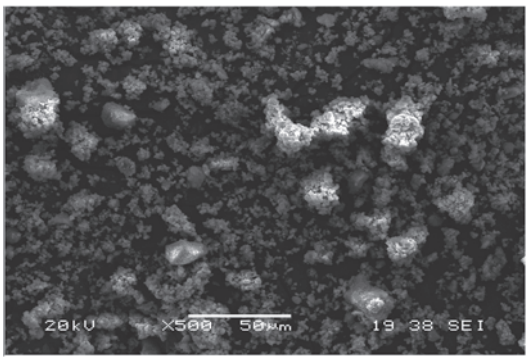

(e)

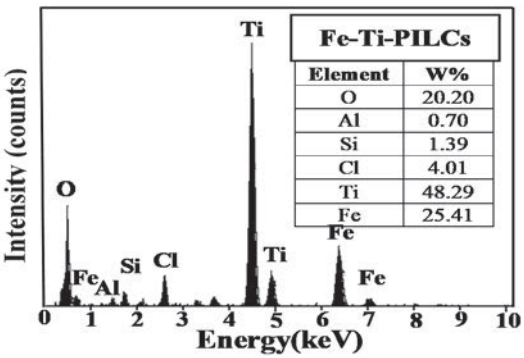

(f)

Fig. 3. SEM images and EDS patterns of zeolite, Fe-Ti-PILCs and Cu-Ti-PILCs: (a) SEM image of zeolite; (b) EDS pattern of zeolite; (c) SEM image of Cu-Ti-PILCs; (d) EDS pattern of Cu-Ti-PILCs; (e) SEM image of Fe-Ti-PILCs; (f) EDS pattern of Fe-Ti-PILCs

The degradation was carried out via produced radical ions from the photocatalytic reactions (Galeano et al., 2014). As shown in Fig. 4, redox reactions were occurred via photocatalytic activity of formed TiO_2 and then, formed radical ions reacted with DB56 and degraded it to carbon dioxide and water.

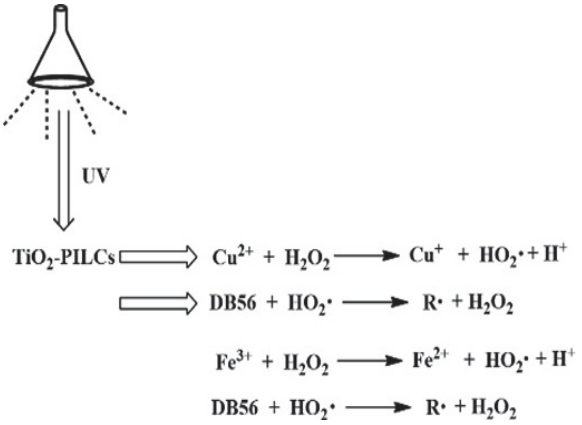

Fig. 4. Possible degradation mechanism

The obtained degradation yields were close using Cu-Ti-PILCs and Fe-Ti-PILCs. In reaction medium, DB56 was adsorbed by PILCs first and then catalytic degradation occurred. The obtained results were close and high using Cu-Ti-PILCs and Fe-Ti-PILCs due to these two effects. The control experiments were carried out in the same experimental conditions except UV light to find adsorption yield. The achieved adsorption rates were 81.3% and 80.1% by using Cu-Ti-PILCs and Fe-Ti-PILCs, respectively. As can be seen from Fig. 5, slightly better results obtained when using Cu-Ti-PILCs in photocatalytic process due to higher dye adsorption efficiency and amount of anatase form of TiO_2. As known, the anatase form of TiO_2 shows a better photocatalytic effect. Another reason that can be mentioned was related to ion exchange step in synthesis proess. The ion exchange between Al and Cu could be better than Al and Fe and thus more radical ions formed by using Cu-Ti-PILCs. Therefore, further studies were performed with Cu-Ti-PILCs.

The effect of H_2O_2 on the degradation of DB56 was investigated by using Cu-Ti-PILCs. As shown at Fig. 6, the removal rates raised by increased H_2O_2 amount especially in the lower time intervals. When excess peroxide was used, more hydroxide radicals were formed rapidly and degradation was occurred in a short time. When less peroxide was used, the hydroxyl radicals required for the complete degradation of hydrocarbon could not formed in a short time. In reaction medium, peroxides also was a product of degradation reaction and during long reaction periods, enough hydroxyl radicals were produced due to mentioned reaction cycle (Fig. 4). If high yields were desired in short time, high amounts of H_2O_2 were required. However, over a long period of time, the use of excess H_2O_2 become unnecessary. The removal rates in 120 min were ~97% and ~100% for 1 mL and 10 mL of H_2O_2 using 1 g of Cu-Ti-PILCs, respectively.

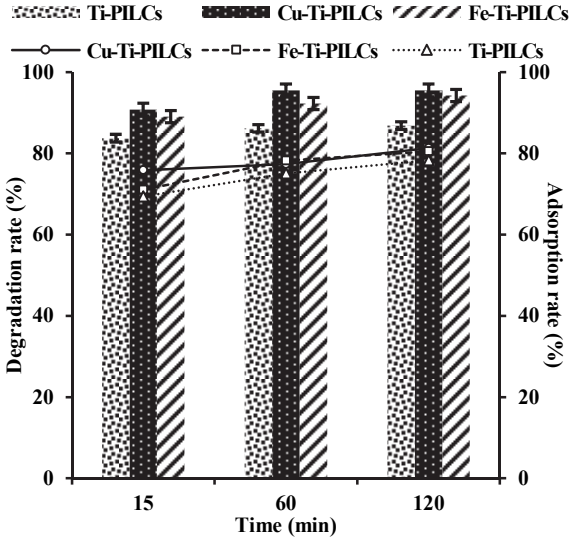

Fig. 5. Removal rates by photocatalytic degradation (Ti-PILCs, Cu-Ti-PILCs and Fe-Ti-PILCs) and adsorption (Ti-PILCs, Cu-Ti-PILCs and Fe-Ti-PILCs) (100 mg/L DB56, 1 g of Cu-Ti-PILCs and Fe-Ti-PILCs, 7.5 mL of H_2O_2)

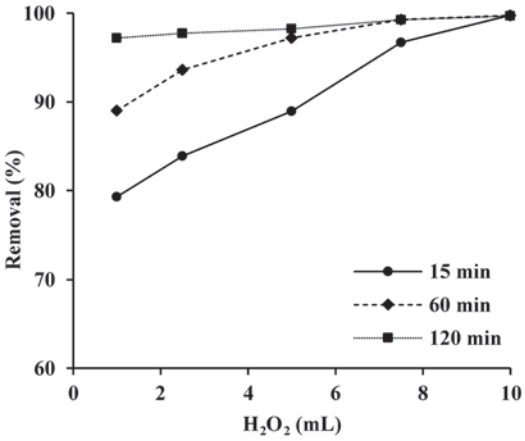

Fig. 6. The effect of H_2O_2 on degradation of DB56 (25 mg/L DB56, 1 g of Cu-Ti-PILCs)

Also, different concentration of dye and amounts of PILCs were tested in order to see the degradation capacity and the results were shown at Figs. 7-8. The increase in dye concentration resulted in small decreases in removal efficiencies. The degradation rate for 10 mg/L dye concentration was ~100% while the value for 100 mg/L was ~95% in 120 min reaction time with the use of 1 mL of H_2O_2 and 1 g of Cu-Ti-PILCs. The effect of amount of Cu-Ti-PILCs was investigated using 100 mg/L DB56. As expected, the removal efficiency increased with raised amount of Cu-Ti-PILCs from 84% to 100% using 0.5

g and 3.0 g, respectively. Increased amount of Cu-Ti-PILCs raised the amount of adsorption. Also, more hydroxyl radicals were produced due to higher reaction yield between photocatalytic material (Cu-Ti-PILCs) and H_2O_2. The photocatalytic degradation process was performed in tap water to see the effect of dissolved ions at the same experiment conditions. The similar result was obtained (~96.5%) from the result in pure water (~97.0%).

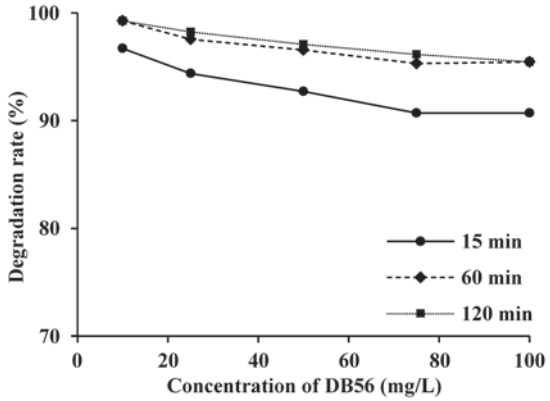

Fig. 7. The degradation rates of DB56 by 1 g of Cu-Ti-PILCs (7.5 mL of H_2O_2)

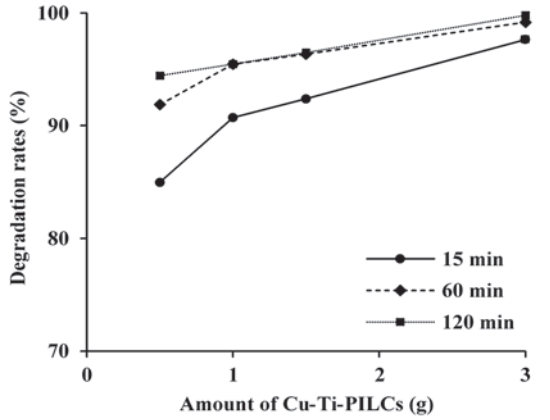

Fig. 8. The effect of amount of Cu-Ti-PILCs (100 mg/L DB56, 7.5 mL of H_2O_2)

The kinetic parameters were calculated by using Lagergren pseudo-first-order (Lagergren, 1898) and pseudo-second-order (Ho and McKay, 1999) equations can be represented as Eqs. (1-2):

$$ln(\ q_e - q_t\ ) = ln\ q_e - k_1 t \quad (1)$$

$$\frac{t}{q_t} = \frac{1}{k_2 q_e^2} + \frac{1}{q_e} t \quad (2)$$

where: q_e (mg/g) is the amounts of solute removed at equilibrium, q_t (mg/g) is the amounts of solute removed at any time(t), k_1 (1/min.) and k_2 (g/mg min.) are the rate constants. The calculated pseudo-first and second-order parameters, and coefficient of determination (R^2) were shown in Table 1. The calculated coefficient of determination for pseudo-second-order model is higher than the pseudo-first-order model and the removal process well fitted with pseudo-second-order kinetic model.

In degradation process, hydroxyl radicals were formed due to photocatalytic activity of Cu-Ti-PILCs. The formed hydroxyl radicals were monitored by the photoluminescence (PL) technique and terephthalic acid (TA) was used as the probing molecule (Islam et al., 2019; Islam et al., 2018). The reaction between hydroxyl radicals and TA resulted in a fluorescent molecule 2-hydroxyterephthalate. This molecule has a fluorescence emission band at 425 nm with an excitation wavelength at 315 nm. In experimental procedure, TA was used instead of DB56 in order to monitoring of formed hydroxyl radical. The florescence spectrum is showed in Fig. 9. The fluorescence intensities of 2-hydroxyterephthalate were increased by the raised amount of formed hydroxyl radicals with time via to catalytic activation. Therefore, the PL results suggested that the Cu-Ti-PILCs photocatalyst generated hydroxyl radicals under the light irradiation.

Table 1. Kinetic parameters

Pseudo-first-order		
q_e (mg/g)	k_1 (1/min.)	R^2
0.7438	0.0316	0.8403
Pseudo-second-order		
q_e (mg/g)	k_2 (g/mg min.)	R^2
0.3797	0.0859	0.9942

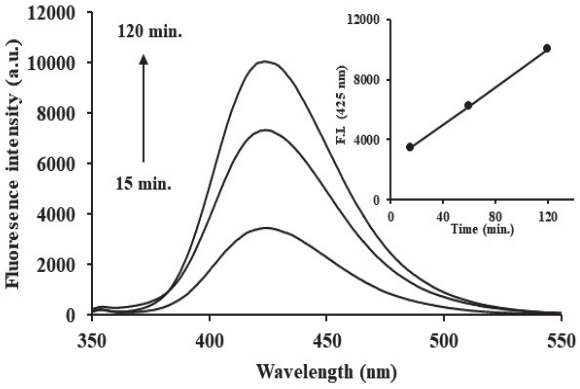

Fig. 9. Time-dependent PL spectra of the 2-hydroxyterephthalic catalyzed by the Cu-Ti-PILCs (5 × 10^{-3} M sodium terephthalate, 1 mL of H_2O_2)

4. Conclusions

In the present study, photocatalytic degradation was evaluated for a dye called DB56 from aqueous solutions by synthesized Cu-Ti-PILCs and Fe-Ti-PILCs. XRD, EDS and FTIR analyzes were performed to prove the content of used zeolite and synthesized structure.

According to the results, better degradation rates were obtained by Cu-Ti-PILCs. This could be attributed to some reasons; (1) better ion-exchange between aluminum and copper than aluminum and

iron, (2) better adsorption to the surface and (3) the amount of formed anatase form of TiO_2. 97% of removal was obtained in 120 min reaction time with using 100 mg/L of dye, 1 g of Cu-Ti-PILCs and 1 mL of H_2O_2. It could be concluded that Cu-Ti-PILCs were an efficient tool for the removal of DB56 from aqueous solutions.

Acknowledgements

This work was financially supported by Sakarya University Commission of Scientific Research Projects (Project number: 2017-02-04-026).

References

Aboelenin R.M.M., Fathy, N.A., Farag, H.K., Sherief, M.A., (2017), Preparation, characterization and catalytic performance of mesoporous silicates derived from natural diatomite: Comparative studies, *Journal of Water Process Engineering*, **19**, 112-119.

Apostolescu G.A., Cernatescu C., Cobzaru C., Tataru-Farmus R.E., Apostolescu N., (2018), Studies on the photocatalytic degradation of organic dyes using CeO_2 - ZnO mixed oxides, *Environmental Engineering and Management Journal*, **14**, 415-420.

Baloyi J., Ntho T., Moma J., (2018), Synthesis and application of pillared clay heterogeneous catalysts for wastewater treatment: a review, *RSC Advances*, **8**, 5197-5211.

Byrappa K., Suresh Kumar B.V., (2007), Characterization of zeolites by infrared spectroscopy, *Asian Journal of Chemistry*, **19**, 4933-4935.

Caliman A.F., Berberidou C., Lazar L., Poulios I., Macoveanu M., (2007), Degradation of Alcian Blue 8 GX by heterogeneous and homogeneous photocatalytic processes, *Environmental Engineering and Management Journal*, **6**, 85-93.

Carriazo J.G., Moreno-Forero M., Molina R.A., Moreno S., (2010), Incorporation of titanium and titanium-iron species inside a smectite-type mineral for photocatalysis, *Applied Clay Scien*ce, **50**, 401-408.

Cysewski P., Jeliński T., (2013), Accuracy of color prediction of anthraquinone dyes in methanol solution estimated from first principle quantum chemistry computations, *Journal of Molecular Modeling*, **19**, 4089-4097.

Dos Santos A.B. Bisschops I.A.E., Cervantes F.J., van Lier J.B., (2005), The transformation and toxicity of anthraquinone dyes during thermophilic (55°C) and mesophilic (30°C) anaerobic treatments, *Journal of Biotechnology*, **115**, 345-353.

Enesca A., Andronic L., Duta A., (2009), Wastewater treatment using optimized TiO_2 photocatalytic properties, *Environmental Engineering and Management Journal*, **8**, 753-758.

Favier L., Simion A.I., Rusu L., Pacala M.L., Grigoras C., Bouzaza A., (2015), Removal of an organic refractory compound by photocatalysis in batch reactor - kinetic studies, *Environmental Engineering and Management Journal*, **14**, 1327-1338.

Fu J, Sheng S., Luo Y., Zhao H., Zeng Q.F., An S.Q, Zhu H.L., (2010), Photo-degradation of C.I. Disperse Blue 56 by UV irradiation combined with manganese minerals, *Water Environment Research*, **82**, 610-616.

Fu J., Ding Y.H., Ma G.Y., Yang J., Zeng Q.F., Liu M.Y., Xia D.S., Zhu H.L., An S.Q., (2009), Removal of a toxic anthraquinone dye by combination of red mud coagulation and ozonation, *Ozone: Science and Engineering*, **31**, 294-300.

Galeano L.A., Vicente M.Á., Gil A., (2014), Catalytic degradation of organic pollutants in aqueous streams by mixed Al/M-pillared clays (M= Fe, Cu, Mn), *Catalysis Reviews*, **56**, 239-287.

Ho Y.S., McKay G., (1999), Pseudo-second order model for sorption processes, *Process Biochemistry*, **34**, 451-465.

Islam Md.T., Dominguez A., Turley R.S., Kim H., Sultana K.A., Shuvo MAI., Alvarado-Tenorio B., Montes M.O., Lin Y., Gardea-Torresdey J., Noveron J.C., (2020), Development of photocatalytic paint based on TiO_2 and photopolymer resin for the degradation of organic pollutants in water, *Science of the Total Environment*, **704**, 135406.

Islam Md.T., Dominguez A., Alvarado-Tenorio B., Bernal R.A., Montes M.O., Noveron J.C., (2019), Sucrose-mediated fast synthesis of zinc oxide nanoparticles for the photocatalytic degradation of organic pollutants in water, *ACS Omega*, **4**, 6560-6572.

Islam Md.T., Jing H., Yang, T., Zubia E., Goos A.G., Bernal R.A., Botez C.E., Narayan M., Chan C.K., Noveron J.C., (2018), Fullerene stabilized gold nanoparticles supported on titanium dioxide for enhanced photocatalytic degradation of methyl orange and catalytic reduction of 4-nitrophenol, *Journal of Environmental Chemical Engineering*, **6**, 3827-3836.

Keshmirizadeh E., Farajikhajehghiasi M., (2014), Decolorization and degradation of Basic Blue 3 and Disperse Blue 56 dyes using fenton Process, *Journal of Applied Chemical Research*, **8**, 81-90.

Khalil M.I., (2015), Co-precipitation in aqueous solution synthesis of magnetite nanoparticles using iron(III) salts as precursors, *Arabian Journal of Chemistry*, **8**, 279-284.

Lagergren S., (1898), About the theory of so called adsorption of soluble substances, *Royal Swedish Academy of Sciences*, **24**, 1-39.

Levine A.D., Meyer M.T., Kish G., (2006), Evaluation of the persistence of micropollutants through pure-oxygen activated sludge nitrification and denitrification, *Water Environment Research*, **78**, 2276-2285.

Mansouri N., Rikhtegar N., Panahi H.A., Atabi F., Shahraki B.K., (2013), Porosity, characterization and structural properties of natural zeolite - clinoptilolite - as a sorbent, *Environment Protection Engineering*, **39**, 139-152.

Mnasri S., Hamdi N., Frini-Srasra N., Srasra E., (2017), Acid-base properties of pillared interlayered clays with single and mixed Zr-Al oxide pillars prepared from Tunisian-interstratified illite-smectite, *Arabian Journal of Chemistry*, **10**, 1175-1183.

Monge-Amaya O., Valenzuela-García J. L., Acedo Félix E., Certucha-Barragán M.T., Leal-Cruz A. L., Almendariz-Tapia F.J., (2013), Biosorptive behavior of aerobic biomass biofilm supported on clinoptilolite zeolite for the removal of copper, *Mineral Processing & Extractive Metallurgy Review*, **34**, 422-428.

Mozgawa W., Krol M., Barczyk K., (2011), FT-IR studies of zeolites from different structural groups, *Chemik*, **65**, 667-674.

Narváez L.E., Rosales-Martínez R.I., Narváez-Hernández L., Hernández- Hernández L.S., Miranda-Vidales J. M., (2015), Electrochemical stability of steel reinforced bars embedded in cement mortars containing clinoptilolite as supplementary, *International Journal of Electrochemical Science*, **10**, 10003-10016.

Parmar N.D., Shukla S.R., (2018), Biodegradation of anthraquinone based dye using an isolated strain

Staphylococcus Hominis Subsp. hominis DSM 20328, *Environmental Progress and Sustainable Energy*, **37**, 203-214.

Simion V.A., Cretescu I., Lutic D., Luca C., Poulios I., (2015), Enhancing the Fenton process by UV light applied in textile wastewater treatment, *Environmental Engineering and Management Journal*, **14**, 595-600.

Stevens R.W., Siriwardane R.V., Logan J., (2008), In situ fourier transform infrared (FTIR) investigation of CO_2 adsorption onto zeolite materials, *Energy and Fuels*, **22**, 3070-3079.

Treacy M.M.J., Higgins J.B., (2001), *Collection of Simulated XRD Powder Patterns for Zeolites*, 4th Edition, John Wiley & Sons, Inc., New York.

Veintemillas-Verdaguer S., Morales M.P., Bomati-Miguel O., Bautista C., Zhao X., Bonville P., Alejo R.P., Ruiz-Cabello J., Santos M., Tendillo-Cortijo F.J., Ferreiros J., (2004), Colloidal dispersions of maghemite nanoparticles produced by laser pyrolysis with application as NMR contrast agents, *Journal of Physics D: Applied Physics*, **37**, 2054-2059.

Volanti D.P., Keyson D., Cavalcante L.S., Simoes A.Z., Joya M.R., Longo E., Varela J.A., Pizani P.S., Souza A.G., (2008), Synthesis and characterization of CuO flower-nanostructure processing by a domestic hydrothermal microwave, *Journal of Alloys and Compounds*, **459**, 537-542.

Wali L.A., Alwan A.M., Dheyab A.B., Hashim D.A., (2019), Excellent fabrication of Pd-Ag NPs/PSi photocatalyst based on bimetallic nanoparticles for improving methylene blue photocatalytic degradation, *Optik - International Journal for Light and Electron Optics*, **179**, 708-717.

Zeng Q.F., Fu J., Shi Y.T., Zhu H.L., (2009), Degradation of C.I. Disperse Blue 56 by ultraviolet radiation/sodium hypochlorite, *Ozone: Science and Engineering*, **31**, 37-44.